Mineralogical Magazine, August 1999, Vol. 63(4), pp. 587–594

Monazite-(Ce)–huttonite solid solutions in granulite-facies metabasites from the Ivrea-Verbano Zone, Italy

H.-J. FÖRSTER AND D. E. HARLOV

GeoForschungsZentrum Potsdam, Telegrafenberg, 14473 Potsdam, Germany

ABSTRACT

Composite populations of monazite-group minerals of both metamorphic and metasomatic origin have been discovered in thin layers of granulite-facies metabasites interlayered with metapelites, located in the Val Strona di Omegna region of the Ivrea-Verbano Zone, Italy. In addition to monazite-(Ce), which is uncommonly poor in Th and is probably formed by incongruent dissolution of apatite, these populations include members of the monazite–huttonite series. The latter minerals contain between 13 and 30.1 mol.% $ThSiO_4$ [= huttonitic monazite-(Ce)], and are known from only half a dozen other occurrences worldwide. We propose that breakdown of primary monazite-(Ce) in the metapelites during granulite-facies metamorphism mobilized Th and the *REE*s, which were then transported by high-grade metamorphic fluids into the metabasite layers to form the Th-rich minerals of the monazite–huttonite series.

KEYWORDS: monazite, huttonite, apatite, crystal-chemistry, granulite-facies metamorphism, metabasite, Ivrea-Verbano Zone.

Introduction

THE light rare-earth element (*LREE*) phosphate mineral monazite typically occurs as an accessory mineral in peraluminous granites, syenitic and granitic pegmatites, carbonatites, as well migmatites, metasediments and metagranitoids (Rosenblum and Fleischer, 1995). Minerals of the monoclinic monazite group have the general formula ABO_4 (A = *REE*, Y, Th, U, Ca, Pb and B = P, Si) and can be classified in the ternary system monazite (*LREE*PO_4)–huttonite ($ThSiO_4$; Pabst and Hutton, 1951)–brabantite [($CaTh(PO_4)_2$; Rose, 1980]. Minerals which are intermediate in composition between end-member monazite and brabantite, and monazite and huttonite, are termed 'cheralite' [(*LREE*,Ca,Th,U)(P,Si)O_4; Bowie and Horne, 1953] and huttonitic monazite (Förster, 1998). The species boundaries in the $2CePO_4$–$2ThSiO_4$–$CaTh(PO_4)_2$ triangle are shown in Fig. 1. Recently, Th-rich brabantitic monazite-(Ce) grains containing up to 53 mol.% $SrTh(PO_4)_2$ were discovered (Chakhmouradian and Mitchell, 1998), further highlighting the enormous compositional diversity within the monazite family of minerals.

While available compositional data indicate complete miscibility in the monazite–brabantite solid-solution series under natural conditions (Förster, 1998), only a few occurrences of Th-rich monazite, plotting at or along the monazite–huttonite join, are currently known (Fig. 1). As a consequence, the assumed continuity of the monazite–huttonite series (Kucha, 1980) is not well demonstrated in nature.

This letter reports compositional data for huttonitic monazite-(Ce) which, together with 'common' monazite-(Ce), has been discovered unexpectedly in granulite-facies metabasites from the Val Strona di Omegna area of the Ivrea-Verbano Zone, northern Italy (see Fig. 1, Franz and Harlov, 1998). Presentation and discussion of the complete set of monazite data produced during an extended and ongoing study of phosphate minerals in granulite- to amphibolite-facies metabasites and metapelitic rocks from that region will be presented in a separate study. Previous electron-microprobe analyses of

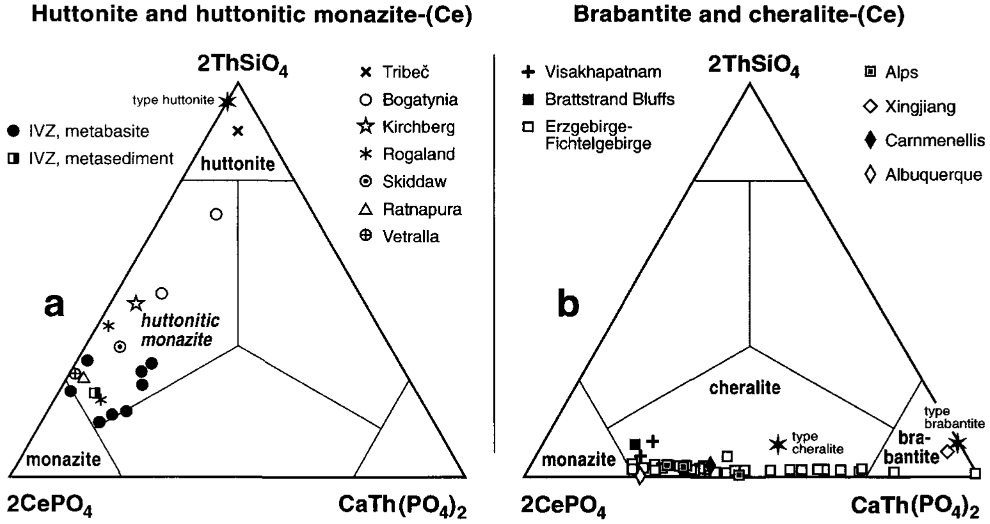

FIG. 1. Occurrences of minerals of the (*a*) huttonite–huttonitic monazite-(Ce) and (*b*) brabantite–cheralite-(Ce) series in the system $2CePO_4$–$2ThSiO_4$–$CaTh(PO_4)_2$ (Bowie and Horne, 1953; Förster, 1998). In calculating end-member proportions, the contents of other *REE* and Y are added to Ce, and the contents of U and Pb are included with the brabantite molecule. See text for localities of and bibliographic references for minerals of the monazite–huttonite series. Type brabantite (Rose, 1980); type cheralite (Bowles *et al.*, 1980); rare-metal pegmatite, Xingjiang, China, (Xianjue, 1978, cited in Fleischer *et al.*, 1981), various Alpine pegmatites (Gramaccioli and Segalstad, 1978; Manucci *et al.*, 1986; Demartin *et al.*, 1991), Carnmenellis two-mica granite, UK (Poitrasson *et al.*, 1996); Albuquerque two-mica granite, Spain (Bea, 1996); granulite-facies metapelitic gneiss, Brattstrand Bluffs, Antarctica (Watt, 1995); granulite-facies hypersthene-bearing granite, Visakhapatnam, India (Kamineni *et al.*, 1991); sillimanite schist, Visakhapatnam (Rao *et al.*, 1997); biotite, two-mica and Li-mica granites, Erzgebirge-Fichtelgebirge, Germany (Förster, 1998; and unpublished data of that author).

monazite have been restricted to those from the metasediments (Schnetger, 1994; Bea, 1996).

Geological background

The Ivrea-Verbano Zone (IVZ) is part of the pre-Alpidic basement of the southern Alps. It consists of a steeply dipping, continuous succession of metamorphic rocks from granulite facies to amphibolite facies. The base of the IVZ (north-western part) is formed by the so-called Mafic Formation (cf. Sinigoi *et al.*, 1994) which itself consists of a succession of granulite-facies metagabbros, metanorites, diorites and ultramafic lenses. The Mafic Formation is overlain by a sequence of interlayered metapelites, metabasites and minor marbles which range in metamorphic grade from granulite to middle amphibolite facies (Henk *et al.*, 1997).

It is commonly postulated that thermal input during the magmatic underplating of the Mafic Formation (*c.* 300 Ma, Vavra *et al.*, 1996) induced granulite facies metamorphism in the overlying rocks and led to partial melting of the metapelitic layers (Schnetger, 1994). Thermobarometric investigations of Henk *et al.* (1997) indicate granulite facies *P-T* conditions of 810±50°C at 8.3±2 kbar near the contact with the Mafic Formation in the northern part of the Val Strona di Omegna. With increasing distance from the contact with the metagabbro, pressure and temperature continuously decrease in the granulite facies terrane reaching temperatures and pressures of 615±30°C and 4.1±1 kbar at the transition to the amphibolite-facies terrane.

Analytical conditions

Minerals of the monazite group were analysed for P, Si, Th, U, *REE* (except Eu and Tm), Y, Al, Fe, Ca and Pb with an automated CAMEBAX SX-50 electron microprobe at the GFZ Potsdam using

TABLE 1. Representative electron-microprobe analyses of monazite-group minerals in metamorphic rocks from the Ivrea-Verbano Zone

Sample	IV94-15	IV94-15	IV94-15	IV94-15	IV97-2a	IV96-181	IV96-181	meta-sediment	IZ96-180a	IV96-181
Analysis	1	2	3	4	5	6	7	8	9	10
P_2O_5	26.5	23.8	21.3	20.4	20.3	22.0	19.4	21.1	29.8	30.3
SiO_2	2.69	4.35	5.70	6.28	6.58	5.47	7.00	4.74	0.38	0.23
ThO_2	16.0	26.8	32.6	35.0	33.4	23.1	29.8	27.3	4.94	n.d.
UO_2	0.37	0.59	0.58	0.59	0.71	0.65	0.87	0.81	0.06	0.08
Y_2O_3	0.08	0.13	0.09	0.09	0.51	n.d.	n.d.	0.96	0.12	n.d.
La_2O_3	13.2	10.1	8.58	8.22	8.79	14.7	11.9	6.43	16.8	14.1
Ce_2O_3	26.8	20.9	18.7	18.0	16.5	24.8	21.7	18.9	30.9	34.3
Pr_2O_3	2.66	2.14	1.94	2.02	1.73	2.06	2.05	2.81	2.95	3.91
Nd_2O_3	9.45	8.14	7.54	7.21	6.92	6.89	6.91	13.6	10.9	14.8
Sm_2O_3	1.11	0.98	0.83	0.81	0.73	0.55	0.51	1.15	1.31	1.58
Gd_2O_3	0.38	0.54	0.34	0.30	0.56	0.22	0.21	0.49	0.56	0.36
Tb_2O_3	0.04	0.08	0.03	n.d.	0.06	0.05	0.03	n.a.	0.08	n.d.
Dy_2O_3	n.d.	0.05	n.d.	n.d.	0.07	n.d.	n.d.	0.46	n.d.	n.d.
Ho_2O_3	n.d.	n.d.	n.d.	n.d.	n.d.	n.d.	n.d.	0.18	n.d.	n.d.
Er_2O_3	n.d.	n.d.	n.d.	n.d.	n.d.	n.d.	n.d.	0.15	n.d.	n.d.
Yb_2O_3	n.d.	n.d.	n.d.	n.d.	n.d.	n.d.	n.d.	0.03	n.d.	n.d.
CaO	1.21	2.38	2.04	1.91	2.33	0.26	0.25	0.41	1.26	0.32
PbO	0.19	0.28	0.39	0.43	0.28	0.30	0.39	n.a.	0.06	0.02
Total	100.7	101.2	100.7	101.2	99.4	101.1	101.0	99.5	100.2	100.0
Mole fractions										
$ThSiO_4$	0.108	0.177	0.240	0.266	0.279	0.229	0.301	0.206	0.015	
$(La\text{-}Sm)PO_4$	0.780	0.629	0.577	0.560	0.535	0.747	0.676	0.678	0.893	0.974
$Y,(Gd\text{-}Lu)PO_4$	0.007	0.012	0.007	0.006	0.021	0.004	0.003	0.041	0.011	0.005
$(Th,Ca,U,Pb)[PO_4]_2$	0.104	0.182	0.176	0.168	0.165	0.020	0.020	0.075	0.081	0.012

n.d. = analysed but not detected, n.a. = not analysed. See text for further explanations.
The analyses 1, 9 and 10 refer to monazite-(Ce), the others to huttonitic monazite-(Ce).
The analyses 1–4 and 6–7 are from zoned grains.

wavelength-dispersive techniques. The operating conditions were as follows: accelerating voltage 20 kV, beam current 40–60 nA, and beam size 1–2 μm. Data reduction, counting times, analysing crystals, standards, analytical precision, and detection limits are described in detail in Förster (1998).

Petrography and composition of huttonitic monazite-(Ce)

Minerals of the monazite group have been identified as widespread accessory phases in thin layers of granulite-facies metabasites (i.e. orthopyroxene-garnet gneisses) from the Val Strona area where they account for a major proportion of the whole-rock *LREE* and Th budgets. These metabasalts (*c.* 46–50 wt.% SiO_2; e.g. Sills and Tarney 1984) are composed of orthopyroxene, clinopyroxene, garnet, plagioclase and quartz with minor K-feldspar, biotite, rutile, ilmenite, zircon, apatite, pyrrhotite and graphite. Monazite is hosted by a variety of major and accessory minerals including garnet, K-feldspar, plagioclase, biotite, quartz, apatite, ilmenite and pyrite and, in general, is distinguished by a large compositional diversity in terms of lanthanide (ΣREE_2O_3 = 34.5–70.1 wt.%) and ThO_2 concentrations (from below the microprobe detection limit to 35 wt.%).

Among those monazite-group minerals, which occur as inclusions in metamorphic garnet or at its grain boundaries, complexly zoned, subhedral to anhedral and commonly corroded grains were observed that are uncommonly rich in Th, specifically in the huttonite component (Fig. 2*a–c*, Table 1). The most Th-rich, patchy domains in these grains of 20–50 μm size have compositions (26.8–35.0 wt.% ThO_2) which identify them as huttonitic monazite-(Ce) in Fig. 1. Grains included in garnet (Table 1, analyses 1–5) also contain substantial amounts of brabantite. They plot at or near the huttonitic monazite–cheralite boundary of the monazite–huttonite–brabantite triangle. In contrast, those occurring at the garnet margin lie close to the monazite–huttonite join (Table 1, analyses 6 and 7). These minerals are compositionally closer to a huttonitic monazite-(Ce) grain which contains 27.3 wt.% ThO_2 (Table 1, analysis 8; Bea, 1996) and comes from a granulite-facies metasediment (i.e. garnet-sillimanite-K-feldspar gneiss) from the same region. However, the latter differs from the huttonitic monazite-(Ce) in the metabasites by having significantly higher concentrations of Nd, Sm, Y and the heavy rare-earth elements (*HREE*).

Diversity in monazite composition is enormous even on the thin-section and grain-size scales. For example, in thin section IV94-15 (cf. Table 1), huttonitic monazite-(Ce) occurs together with a less Th-rich monazite grain in the same garnet crystal (Fig. 2*a–c*). Monazite in K-feldspar and quartz contains between 2 and 4 wt.% ThO_2. Monazite grains observed principally in apatite (Fig. 2*d*), but also occasionally in biotite and pyrite, have Th concentrations below the microprobe detection limit.

Occurrences of huttonite and huttonitic monazite-(Ce)

Huttonitic monazite-(Ce) and, even less likely, the huttonite end-member are rarely found in nature (Fig. 1). Huttonite confirmed by X-ray data has been described only once, from its type locality, Gillespie's Beach, New Zealand, where it occurs as minute grains in a beach sand and contains 76.6 wt.% ThO_2 (Pabst and Hutton, 1951). Recently, Broska *et al.* (1998) identified a thorium silicate mineral (77.2 wt.% ThO_2) in S-type biotite granodiorites from the Tribeč Mts. (Slovakia), which displays an uncommonly shaped *LREE* pattern and is assumed to represent huttonite rather than thorite.

The currently known occurrences of huttonitic monazite-(Ce) are: (1) granitic pegmatites of Bogatynia, Poland (ThO_2 = 56.4–69.9 wt.%; Kucha, 1980); (2) the Kirchberg granite, Germany (41.8 wt.% ThO_2; Förster, 1998); (3) amphibolite-facies calc-alkaline granitic augen gneisses (34.2 wt.% ThO_2) and granulite-facies charnockitic gneisses (22.7 wt.% ThO_2) from the Rogaland-Vest Agder terrain, SW Norway (Bingen and van Breemen, 1998); (4) the Skiddaw granite, NW England (28.9 wt.% ThO_2; Poitrasson *et al.*, 1996); (5) a pebble from Ratnapura, Sri Lanka (28.2 wt.% ThO_2; Pabst and Hutton, 1951); and (6) a holocrystalline ejectum from Vetralla, Italy (27.1 wt.% ThO_2; Della Ventura *et al.*, 1996).

The rare occurrence of huttonite is suggested to be the result of its instability, with respect to its tetragonal analogue thorite, at pressures and temperatures normally encountered under high-grade conditions in the Earth's crust (Dachille and Roy, 1964). Specifically, huttonite should not be stable at the pressures and temperatures under which the granulite-facies metabasites and metapelites of the IVZ formed ($T = 600-800°C$, $P = 6-8$ kbar). However, substitutions of *REE*PO_4 and $CaTh(PO_4)_2$ appear to increase the huttonite stability field considerably, thus permitting formation of huttonitic monazite-(Ce) at these *P-T* conditions.

Discussion and geological implications

Extended compositional variability and the internal textural structure of monazite grains from granulite-facies metabasites of the Ivrea-Verbano Zone are consistent with the observation that this particular mineral typically underwent several growth and resorption episodes under high-grade metamorphic conditions, resulting in a series of composite populations (e.g. Zhu *et al.*, 1997; Bingen and van Breemen, 1998; Braun *et al.*, 1998; Cocherie *et al.*, 1998; Hawkins and Bowring, 1999).

Generally, formation of monazite as a primary (igneous) mineral is incompatible with the basaltic nature of its host rock, in which major minerals such as amphiboles, pyroxenes and garnet normally account for the bulk of the lanthanides and actinides. Logically, the crystallization of monazite in these metabasites should be secondary, and is probably linked to contact-metamorphic overprinting and associated high-grade fluid flow (e.g. Franz and Harlov, 1998), which has been suggested to have affected the mafic rocks during emplacement of the Mafic Formation and subsequent granulite-facies metamorphism. High-grade metamorphic and metasomatic processes, involving both internal and external sources of the *REE*s, are also proposed to account for the few other occurrences of monazite in mafic-ultramafic rocks known to date (Rudnick *et al.*, 1993; Liou and Zhang, 1996).

Monazite-group minerals are present only in granulite-facies metabasites which form thin layers or lenses (25–100 cm thick) and are complexly interfolded with the metasediments. In contrast, monazite is apparently absent from amphibolite-facies metabasites that form thick units (20–100 m) interbanded with amphibolite-facies garnet-biotite gneisses. These observations imply that both the elevated *P-T* conditions required for granulite-facies metamorphism and the small thickness of the basaltic layers in immediate contact with the monazite-bearing metapelites are critical for the formation of monazite. These observations support present models involving a high degree of mobility of the *REE* and the actinides during granulite-facies metamorphism (e.g. Pan and Fleet, 1996).

A number of potential sources for the *REE*s and the actinides in the different populations of monazite must be considered, including pre-existing *REE*-bearing minerals both within the granulite-facies metabasite itself and the inter-layered metapelites. Monazite with high concentrations of Th and U, including the huttonitic monazite-(Ce) discussed herein, are probably produced partially or wholly by the breakdown of Th-bearing monazite-(Ce) in the immediate adjacent metasediments (Table 1, analysis 9), with subsequent large-scale, high-grade fluid flow-induced redistribution of the now mobile lanthanide and actinide elements into the metabasites. Significant enrichment in *REE*, other high field-strength elements and phosphorus in the granulite-facies metabasalts, in comparison with the amphibolite-facies metabasalts, is suggested to be the result of the introduction of elements from external source(s) and does not represent a primary signature as proposed by Sills and Tarney (1984). Thus, current ideas on the nature of the basaltic magmatism in the IVZ, which invoke a different petrogenesis and tectonic position for type 1 and 2 amphibolites (Sills and Tarney, 1984), might require some revision.

The Th-rich monazite grains are considered to have crystallized earlier than, or simultaneously with their host minerals, identifying them as metamorphic in origin. In distinct compositional and textural contrast to these monazites are tiny monazite microcrystals (<1–2 μm) inside apatite and somewhat larger anhedral, homogeneous grains on the apatite surface that are strongly enriched in *REE* but extremely poor in both Th and U (Table 1, analysis 10). These specific compositions are in accordance with those obtained from previous studies of phosphate minerals from various high-grade metamorphic rocks (Åmli, 1975; Pan and Fleet, 1993; Pan, 1997; Hiroi *et al.*, 1997), suggesting that monazite, which occurs in or at the surface of apatite, shares the common feature of containing Th (but not necessarily U) in concentrations $\ll 1$ wt.%, typically at or below their microprobe detection limits. Thus, in metamorphic rocks, extremely Th-poor monazite might be used to fingerprint its potential sources which comprise allanite and titanite as well as leaching or replacement of fluorapatite (e.g. Pan, 1997). It could be used specifically in igneous rocks to

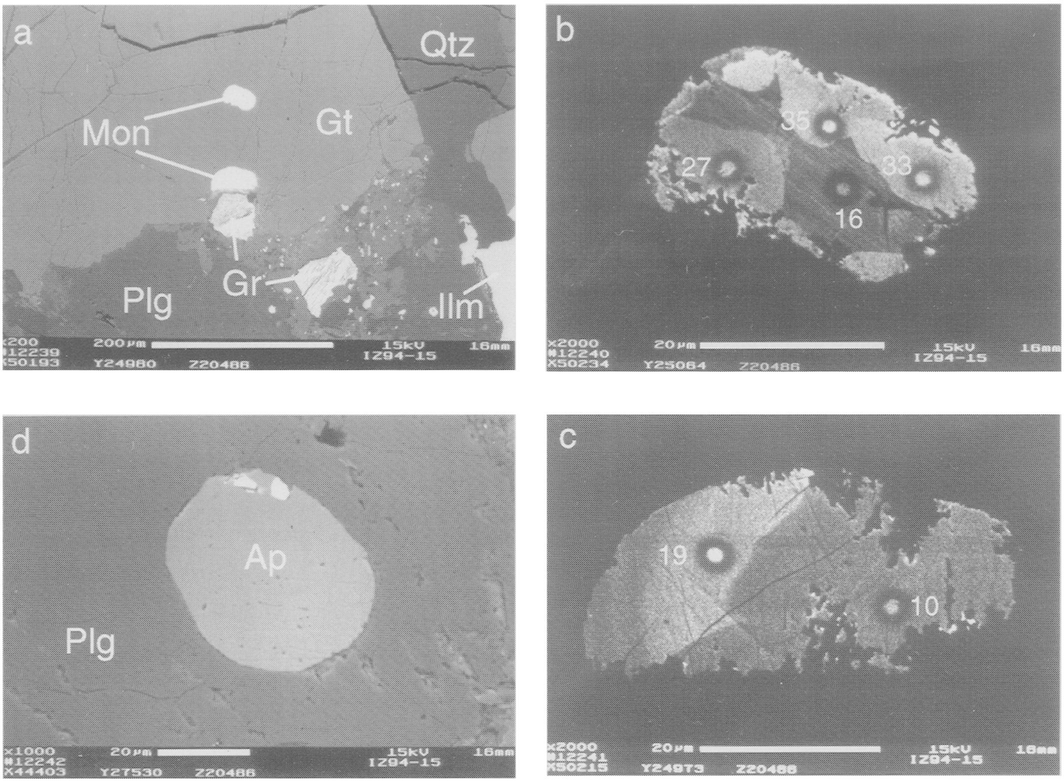

FIG. 2. (*opposite*) Back-scattered electron microscope images of compositionally and texturally distinct monazite grains in thin section IV94-15. The numbers at the locations of the EPMA analyses refer to the measured ThO_2 concentrations (in wt.%). Qtz = quartz, Gt = garnet, Plg = plagioclase, Gr = graphite, Ilm = ilmenite, Mon = monazite, Ap = apatite. (*a*) Th-rich monazite-(Ce) grains in garnet. (*b*) Huttonitic monazite-(Ce) showing sector zoning. The internal zoning of the crystal reveals local truncations of growth zones throughout the growth history. This texture is interpreted to reflect a cyclic history of growth and dissolution during metamorphism, resulting from variations in the composition of the surrounding pore fluids. (*c*) Heterogeneously zoned grain of Th-rich monazite-(Ce). (*d*) Small Th-poor monazite-(Ce) inclusions at the upper margin of an apatite crystal.

distinguish between monazite formed by incongruent dissolution of apatite during rock anatexis (e.g. Wolf and London, 1995) and monazite grown from a melt. The latter commonly contain Th in excess of 2–4 wt.% (e.g. Förster, 1998).

Thorium depleted monazite is not restricted in occurrence to apatite but, very occasionally, was also observed in plagioclase, quartz, ilmenite, and pyrite on the thin-section scale. If apatite is also assumed as the ultimate source of the *REE*s in these monazite grains, mobilization of the *REE*s during breakdown or replacement of apatite must have occurred at least over distances of millimetres or centimetres.

Monazites from the metabasites are compositionally distinct from those occurring in the intimately associated metasediments. Monazite from the latter displays a restricted range in composition, with *REE* patterns and ThO_2 contents of 2.1–8.1 wt.% typical for minerals of metamorphic origin. These observations indicate that the monazite grains found in the mafic rocks are not simply mechanical admixtures from the metasediments taken up by the basaltic melts during interaction with the sedimentary rocks.

A more detailed picture of monazite formation in the granulite-facies metabasites will help to further explain the observed strong spatial relations of compositionally distinct monazite grains to a particular host or suite of host phases. No convincing explanation can yet be given as to whether the apparent association of huttonitic monazite-(Ce) with garnet is accidental or not. Furthermore, the presence of monazite and its specific compositional signatures should provide important insights into the cooling history of the IVZ metamorphic complex (based on Th-U-total Pb ages) after emplacement of the basal ultramafic melts (Mafic Complex) as well as allow conclusions on the origin of the monazite host minerals. All these issues will be addressed in a forthcoming, more extended paper.

Acknowledgements

The authors wish to thank O. Appelt (Potsdam) for her valuable assistance with the electron microprobe analyses. Reviews by G. Della Ventura and an anonymous referee helped to improve the manuscript. I. Broska (Bratislava) kindly provided a copy of his paper on huttonite which was published in *Mineralia Slovaca*.

References

Åmli, R. (1975) Mineralogy and rare earth geochemistry of apatite and xenotime from the Gloserheia granite pegmatite, Froland, southern Norway. *Amer. Mineral.*, **60**, 607–20.

Bea, F. (1996) Residence of *REE*, Y, Th and U in granites and crustal protoliths; Implications for the chemistry of crustal melts. *J. Petrol.*, **37**, 521–52.

Bingen, B. and van Breemen, O. (1998) U-Pb monazite ages in amphibolite- to granulite-facies orthogneiss reflect hydrous mineral breakdown reactions: Sveconorwegian Province of SW Norway. *Contrib. Mineral. Petrol.*, **132**, 336–53.

Bowie, S.H.U. and Horne, J.E.T. (1953) Cheralite, a new mineral of the monazite group. *Mineral. Mag.*, **30**, 93–99.

Bowles, J.F.W., Jobbins, E.A. and Young, B.R. (1980) A re-examination of cheralite. *Mineral. Mag.*, **43**, 885–8.

Braun, I., Montel, J.-M. and Nicollet, C. (1998) Electron microprobe dating of monazites from high-grade gneisses and pegmatites of the Kerala Khondalite Belt, southern India. *Chem. Geol.*, **146**, 65–85.

Broska, I., Petrik, I. and Siman, P. (1998) Accessory huttonite and two types of allanite in Tribeč S-type granitoids (in Czech). *Miner. Slovaca*, **30**, 311–4.

Chakhmouradian, A.R. and Mitchell, R.H. (1998) Lueshite, pyrochlore and monazite-(Ce) from apatite-dolomite carbonatite, Lesnaya Varaka complex, Kola Peninsula, Russia. *Mineral. Mag.*, **62**, 769–82.

Cocherie, A., Legendre, O., Peucat, J.J. and Kouamelan, A.N. (1998) Geochronology of polygenetic monazites constrained by *in situ* electron microprobe Th-U-total lead determination: Implications for lead behaviour in monazite. *Geochim. Cosmochim. Acta*, **62**, 2475–97.

Dachille, F. and Roy, R. (1964) Effectiveness of shearing stresses in accelerating solid phase reactions at low temperatures and high pressures. *J. Geol.*, **72**, 243–7.

Della Ventura, G., Mottana, A., Parodi, G.C., Raudsepp, M., Bellatreccia, F., Caprilli, E., Rossi, P. and Fiori, S. (1996) Monazite-huttonite solid-solutions from the Vico Volcanic Complex, Latium, Italy. *Mineral. Mag.*, **60**, 751–8.

Demartin, F., Pilati, T., Diella, V., Donzelli, S. and Gramaccioli, C.M. (1991): Alpine monazite: further data. *Canad. Mineral.*, **29**, 61–7.

Fleischer, M., Chao, G.Y. and Francis, C.A. (1981) New mineral names. *Amer. Mineral.*, **66**, 878–9.

Förster, H.-J. (1998) The chemical composition of REE-Y-Th-U-rich accessory minerals in peraluminous granites of the Erzgebirge-Fichtelgebirge region, Germany. Part I: The monazite-(Ce)–brabantite solid solution series. *Amer. Mineral.*, **83**, 259–72.

Franz, L. and Harlov, D.E. (1998) High-grade K-feldspar veining in granulites from the Ivrea-Verbano Zone, northern Italy: fluid flow in the lower crust and implications for granulite facies genesis. *J. Geol.*, **106**, 455–72.

Gramaccioli, C.M. and Segalstad, T.V. (1978) A uranium- and thorium-rich monazite from a south-Alpine pegmatite at Piona, Italy. *Amer. Mineral.*, **63**, 757–61.

Hawkins, D.P. and Bowring, S.A. (1999) U-Pb monazite, xenotime and titanite geochronological constraints on the prograde to post-peak metamorphic thermal history of Paleoproterozoic migmatites from the Grand Canyon, Arizona. *Contrib. Mineral. Petrol.*, **134**, 150–69.

Henk, A., Franz, L., Teufel, S. and Oncken, O. (1997) Magmatic underplating, extension, and crustal reequilibration: insights from a cross-section through the Ivrea Zone and Strona-Ceneri Zone, northern Italy. *J. Geol.*, **105**, 367–77.

Hiroi, Y., Motoyoshi, Y., Shiraishi, K. and Mathavan, V. (1997) Local formation of hercynite-plagioclase symplectite after garnet and sillimanite in khondalite from Habarana, Sri Lanka; mineral textures. In: *Proc. 16th NIPR Symp.: Antarctic Research* (Funaki, M., ed.), Nat. Inst. of Polar Research, Tokyo, 153–64.

Kamineni, D.C., Rao, A.T. and Bonardi, M. (1991) The geochemistry of monazite types from Eastern Ghats granulite terrain, India. *Mineral. Petrol.*, **45**, 119–30.

Kucha, H. (1980) Continuity in the monazite-huttonite series. *Mineral. Mag.*, **43**, 1031–4.

Liou, J.G. and Zhang, R.Y. (1996) Petrogenesis of ultrahigh-*P* garnet-bearing ultramafic rocks from Maowu, the Dabie Mountains, central China. *Geol. Soc. Amer., Abstr. with Programs*, **28**, 69.

Mannucci, G., Diella, V., Gramaccioli, C.M. and Pilati, T. (1986) A comparative study of some pegmatitic and fissure monazite from the Alps. *Canad. Mineral.*, **24**, 469–74.

Pabst, A. and Hutton, C.O. (1951) Huttonite, a new monoclinic thorium silicate, with an account on its occurrence, analysis, and properties. *Amer. Mineral.*, **36**, 60–9.

Pan, Y. (1997) Zircon- and monazite-forming metamorphic reactions at Manitouwadge, Ontario. *Canad. Mineral.*, **35**, 105–18.

Pan, Y. and Fleet, M.E. (1993) Oriented monazite inclusions in apatite porphyroblasts from the Hemlo gold deposit, Ontario, Canada. *Mineral. Mag.*, **57**, 697–707.

Pan, Y. and Fleet, M.E. (1996) Rare earth element mobility during prograde granulite facies metamorphism: significance of fluorine. *Contrib. Mineral. Petrol.*, **123**, 251–62.

Poitrasson, F., Chenery, S. and Bland, D.J. (1996) Contrasted monazite hydrothermal alteration mechanisms and their geochemical implications. *Earth Planet. Sci. Lett.*, **145**, 79–96.

Rao, A.T., Fonarev, V.I., Konilov, A.N. and Romanenko, I.M. (1997) Cheralite from Visakhapatnam area in the Eastern Ghats granulite belt, India. *Gondwana Res.*, **1**, 137–41.

Rose, D. (1980) Brabantite, CaTh$[PO_4]_2$, a new mineral of the monazite group. *Neues Jahrb. Mineral. Mh.*, 247–57.

Rosenblum, S. and Fleischer, M. (1995) The distribution of rare-earth elements in minerals of the monazite family. *U.S. Geol. Surv. Bull.*, No. **2140**, 1–62.

Rudnick, R.L., McDonough, W.F. and Chappell, B.W. (1993) Carbonatite metasomatism in the northern Tanzanian mantle: petrographic and geochemical characteristics. *Earth Planet. Sci. Lett.*, **114**, 463–75.

Schnetger, B. (1994) Partial melting during the evolution of the amphibolite- to granulite facies gneisses of the Ivrea Zone, northern Italy. *Chem. Geol.*, **113**, 71–101.

Sills, J.D. and Tarney, J. (1984) Petrogenesis and tectonic significance of amphibolites interlayered with meteasedimentary gneisses in the Ivrea Zone, southern Alps, northwest Italy. *Tectonophys.*, **107**, 187–206.

Sinigoi, S., Quick, J.E., Clemens-Knott, D., Mayer, A., Demarchi, G., Mazzuchelli, M., Negrini, L. and Rivalenti, G. (1994) Chemical evolution of a large mafic intrusion in the lower crust, Ivrea-Verbano Zone, northern Italy. *J. Geophys. Res.*, **99**, 21,575–90.

Vavra, G., Gebauer, D., Schmid, R. and Compston, W. (1996) Multiple zircon growth and recrystallization during polyphase Late Carboniferous to Triassic metamorphism in granulites of the Ivrea Zone (southern Alps): an ion microprobe (SHRIMP) study. *Contrib. Mineral. Petrol.*, **122**, 337–58.

Watt, G.R. (1995) High-thorium monazite-(Ce) formed during disequilibrium melting of metapelites under granulite-facies conditions. *Mineral. Mag.*, **59**, 735–43.

Wolf, M.D. and London, D. (1995) Incongruent dissolution of REE- and Sr-rich apatite in peraluminous granitic liquids: Differential apatite, monazite, and xenotime solubilities during anatexis. *Amer. Mineral.*, **80**, 765–75.

Zhu, X.K., O'Nions, R.K., Belshaw, N.S. and Gibb, A.J. (1997) Significance of in situ SIMS chronometry of zoned monazite from the Lewisian granulites, northwest Scotland. *Chem. Geol.*, **135**, 35–53.

[*Manuscript received 5 November 1998:*
revised 5 May 1999]